Active and passive monitoring of fault reactivation under stress cycling

Naderloo, M.; Veltmeijer, A.V.; Barnhoorn, A.

DOI
10.1190/image2022-3750358.1

Publication date
2022

Document Version
Final published version

Published in
Second International Meeting for Applied Geoscience & Energy

Citation (APA)
Naderloo, M., Veltmeijer, A. V., & Barnhoorn, A. (2022). Active and passive monitoring of fault reactivation under stress cycling. In A. Abubakar , & A. Hakami (Eds.), *Second International Meeting for Applied Geoscience & Energy* (Vol. 2022-August, pp. 1576-1580). (SEG Technical Program Expanded Abstracts). https://doi.org/10.1190/image2022-3750358.1

Active and Passive Monitoring of Fault Reactivation under Stress Cycling

Milad Naderloo[1], Aukje Veltmeijer[1,], Auke Barnhoorn[1]. [1] Delft University of Technology*

Summary

Increased seismicity, due to subsurface activities has led to increased interest in monitoring and seismic risk mitigation. In this study we combined passive and active acoustic monitoring methods to monitor fault sliding and reactivation in the laboratory. Acoustic emission (AE) and ultrasonic transmission measurements were performed during stress-cycling to monitor stress-driven fault reactivation. We show the use of the transmissivity and coda wave interferometry of the active acoustic measurements and the number of generated AE events for fault reactivation monitoring. Combining these two methods, we are able to detect the different phases of fault reactivation process under stress cycling including, early aseismic creep (pre-slip), fault slip, and continuous sliding. Combining both active and passive monitoring increases accuracy of monitoring and can lead to better seismic risk mitigation

Introduction

Increasing human activities in the subsurface, due to rising energy demand, and the demand for renewable energy have led to an increase in induced seismicity all over the world. Seismicity is recorded at different subsurface-related projects, such as water waste injection, gas extraction, and geothermal energy production sites. A well-known example is the M5.4 earthquake in Pohang (Kim et al., 2018), or the high number of seismicity recordings in Groningen, caused by gas extraction (Van Thienen-Visser & Breunese, 2015).

Monitoring and seismic risk mitigation have received much interest over the years. Multiple studies have been conducted to improve the monitoring system of induced seismicity (Mahani et al., 2016; Grigoli et al., 2017; Eaton, 2018). Verdon et al (2010), showed there is a correlation between the seismicity rate with injection rate and the production activities using passive monitoring. Using improved matching and locating techniques, Chen et al (2018) showed better detection of the seismicity events and the clustering of seismic activity caused by the pre-existing faults and fractures with passive monitoring.

Monitoring induced seismicity, however, still poses a number of challenges, including the need for near-real-time monitoring and limitations associated with seismic network quality (Grigoli et al., 2017). For improving monitoring and managing system of induced seismicity, combining geophysical, geological, and hydrological data from the field with modelling is required. Potential seepage or leakage along faults or fracture zones was studied by Oye et al (2021), using both active and passive monitoring techniques. Similarly, active monitoring techniques are used to monitor changes in the subsurface prior to fault reactivation. Laboratory studies have shown the sensitivity of ultrasonic P-waves to the reactivation of faults for frictional sliding experiments (Kaproth and Marone, 2013; Shreedharan et al., 2021). Also at larger scale, precursory signals can be observed using active acoustic monitoring. Chiarabba et al., 2020 observed at a larger (crustal) scale an increase, and near the hypocentre, a decrease in P-wave velocity before an M6.5 in Italy.

Most of the studies in field or laboratory scale are based on either passive monitoring or active monitoring, only a limited number combine both techniques It can be valuable and helpful for monitoring purposes to combine the active and passive acoustic methods.
This study aims to shed light on using both passive and active acoustic methods for monitoring fault sliding under stress cycling on laboratory scale We perform stress-driven fault reactivation experiments on sandstones under stress cycling.

Method

In this study, high porosity Red Pfaelzer sandstones were used, these are analog to the Rotliegend sandstones of the Groningen gas reservoir (in the north of the Netherlands). The cylindrical core samples were cut at an angle of 30° angle to the vertical cylinder axis to simulate a fault plane. The samples, including saw cut had dimensions of 30 ± 0.5 mm in diameter and 70 ± 2 mm in length. A gas expansion (Helium) pycnometer was used to determine the average connected porosity of the samples: 19-20%.

We used an instrumented Hoek cell in a 500kN uniaxial loading machine (Figure 1). A three-step stress-driven protocol for fault reactivation was performed (Figure 2).

1. During the first step, axial stress and confining pressure increased hydrostatically up to the desired confining pressure of 20 MPa, while the sample was fully saturated.
2. During the second step, axial stress is increased to reach the pre-determined shear strength of the fault plane (the reactivation zone).
3. In step three, the cyclic reactivation scenario was performed in which after fault slip, axial stress ($\sigma 1$) was decreased with 12 MPa and afterwards increased again up to the previous stress (Figure 2).

Active and Passive Monitoring of Fault Reactivation under Stress Cycling

Two sets of acoustic experiments were performed during stress-driven cyclic fault reactivation. Reactivation with passive acoustic emission (AE) monitoring and reactivation with active acoustic monitoring.

The active acoustic monitoring was performed using ultrasonic transmission measurements. Two P-wave transducers are integrated into the pistons in the loading system (Figure 1), with the source at the top and the receiver at the bottom of the sample. The transducers have a peak operating frequency of 1 MHz, and every 2 seconds, 512 P-waves were sent, recorded, and stacked to reduce the signal-to-noise ratio. The transmission data was analysed using the transmissivity: $T = |A_{max}|$, which is the maximum amplitude of the recorded P-wave. Additionally, coda wave interferometry (CWI) (Snieder, 2006) is used to monitor the change in velocity (dv/v) between two consecutive recorded waves. Using a moving reference wavefield for the CWI, the changing medium is continuously monitored (Zotz-Wilson et al., 2019).

The passive acoustic monitoring (AE) was performed using an array of 10 piezo-ceramic transducers (Figure 1) to detect micro-seismic events. The AE transducers are 5mm in diameter, with a dominant resonant frequency of about 1 MHz, and the signals were amplified using pre-amplifiers. The continuous recorded waveform data was cut into single waveforms (AE events) for further analysis, using a pre-defined trigger logic. These AE events were stored if, in five or more transducers, the waveforms recorded exceeds a voltage threshold of 25mV, within a time window of 480 points and a sampling rate of 2 MHz.

Discussion of Results

In total, 9 stress-reactivation cycles were performed, including acoustic monitoring (Figure 2). The stress-driven fault reactivation cycles can be divided into three parts. 1. stress increase, consisting of pre-slip phase and the fault reactivation phase. 2. constant sliding (pure fault slip), in which the sample was continued to be stressed, but constant fault slip counteracted this increase resulting in a more or less constant stress, and 3. stress decrease, after which a new cycle begins.

Figure 3 shows the AE results, the axial stress (σ1), micro-seismic event amplitude and cumulative events are shown. A silence zone, showing zero generated AE event is caused by reducing the stress after fault slip. However, by increasing the stress, AE events starts to appear before exceeding previous reached maximum stress (maximum stress from previous cycle) and before pure fault slip. AE events are generated from 97% of the maximum stress indicating the fault reactivation (Figure 3).

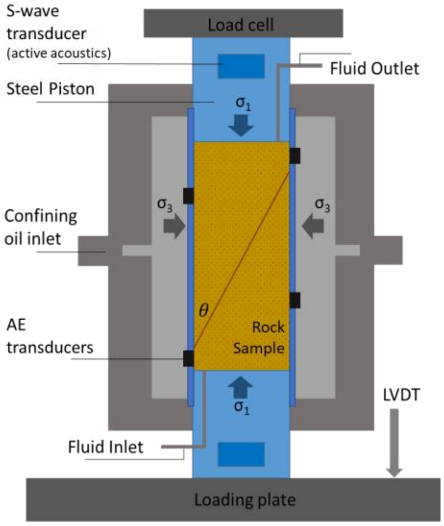

Figure 1: Schematic illustration of instrumented Hoek cell with AE sensors, and S-wave transducers. The shortening of the sample was recorded with two linear variable displacement transducers (LVDT's)

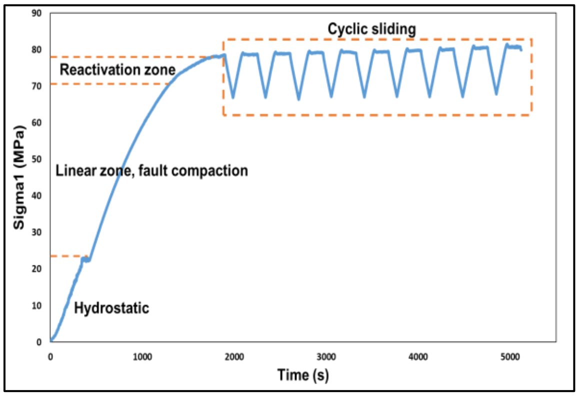

Figure 2: Axial stress ($\sigma 1$) as a function of time. Different phases of fault reactivation experiment; hydrostatic, linear zone, reactivation zone, and cyclic sliding.

Prior to fault reactivation and pure fault slip, a pre-slip aseismic stage is present. During this pre-slip phase, the fault plane experiences creep (slow slip). During this stage the stress continues to build up, but shows a deviation from the linear increase (Figure 3, beige and blue colour). During this pre-slip phase (blue colour), low amplitude AE events (and a lower event rate) were recorded. After this phase, stress reaches its maximum value and then it drops, indicating fault reactivation.

During reactivation (Figure 3, green zone), the event rate and maximum amplitude for the individual AE events increase. After reactivation, we observe continuous sliding (pure slip). During this phase (Figure 3, grey zone), continuous micro-seismic generation can be observed.

Figure 4 shows the data from active acoustic monitoring. Shown is the axial stress (σ1), the cumulative velocity change ($[\mathrm{dv/v}]_{sum}$) obtained by CWI, and the transmissivity (T). The velocity and transmissivity show an overall decreasing trend, but within each cycle the different phase of fault reactivation can be identified. $[\mathrm{dv/v}]_{sum}$ and T, show an approx.. linear increase due to the imposed increasing stress (Figure 4, beige zone). Before early creep phase (or before 95% of maximum stress), strain is slowly accumulating on fault plane and stress is building up, however, this stress is not enough to overcome the shear strength, thus the fault remains locked and the contact area between the two sides of fault increases (the asperities lock). This results in an constant (linear) increase of T and $[\mathrm{dv/v}]_{sum}$ with increasing pressure and micro-seismic events are not generated.

Before fault reactivation, both $[\mathrm{dv/v}]_{sum}$ and T show a deviation from their linear increase. This coincides with the early creep phase (aseismic stage) and this reduction is attributed to pre-slip and dilation (Kaproth and Marone, 2013; Shreedharan et al., 2021). During this aseismic phase, the contact area along the fault plane, or the asperities, are slowly destroyed, resulting in a reduction of T and $[\mathrm{dv/v}]_{sum}$. The detection of the early creep phase using T and $[\mathrm{dv/v}]_{sum}$ is at 95% of the maximum stress indicating the fault reactivation. After fault reactivation (stress drop) both parameters show a constant decrease, consistent with the continuous sliding and the continuous destruction of asperities along the fault plane.

Both the passive data and active data shows, we can detect the early creep phase (aseismic stage), the fault reactivation (stress drop), and the continuous sliding phase. Therefore, both methods can be used as a monitoring method of pre-slip and can act as precursory signals to imminent fault slip.

The active monitoring shows precursory signal to fault slip from 95% to failure, whereas the passive (AE) method shows the first recorded events from 97% to failure. The active monitoring is independent of generated seismicity and can be deployed and used for monitoring at any stage of reactivation. Passive monitoring can provide valuable insight in the location and moment tensor of the fault reactivation and generated seismicity. Therefore, these methods complement each other and monitoring can be improved.

One of the most used strategies for seismicity risk mitigation is the traffic light system (TLS), in which an injection protocol is modified by flow rate or fluid pressure based on pre-defined thresholds of seismic magnitudes or other factors ((Hofmann et al., 2018). The typical observable variables used for TLS decision-making are magnitude, peak ground velocity or peak ground acceleration, and the rate of events ((Muntendam-Bos et al., 2022). Thus, using active acoustic analysis next to passive can greatly improve the monitoring accuracy and can benefit TLS.

Conclusion

In this study, we used the passive and active acoustic techniques to monitor stress-driven fault reactivation experiments under stress cycling.

1. We showed that both passive acoustic (acoustic emission) and active acoustic monitoring can be used to detect fault reactivation process under stress cycling which includes different phases; linear strain build up, early creep (pre-slip), stress drop (main slip), and continuous sliding phase.

2. The active acoustic technique detected the early creep phase at 95% before failure, and AE at 97% before failure. The active methods are earlier and slightly more sensitive, and are independent of seismicity generated movement along the fault. Therefore, combination of both method can be beneficial to increase accuracy of monitoring.

These results have shown that monitoring fault reactivation in the laboratory with the active and passive techniques is feasible. As a result, the combination of passive and active techniques may be useful for monitoring faulted or critical stressed reservoirs that undergoing cyclic stress behaviour.

Acknowledgements

We like to thank the laboratory staff of the TU Delft for their support, especially Marc Friebel. This research was (partially) funded by NWO Science domain (NWO-ENW), project DEEP.NL.2018.048

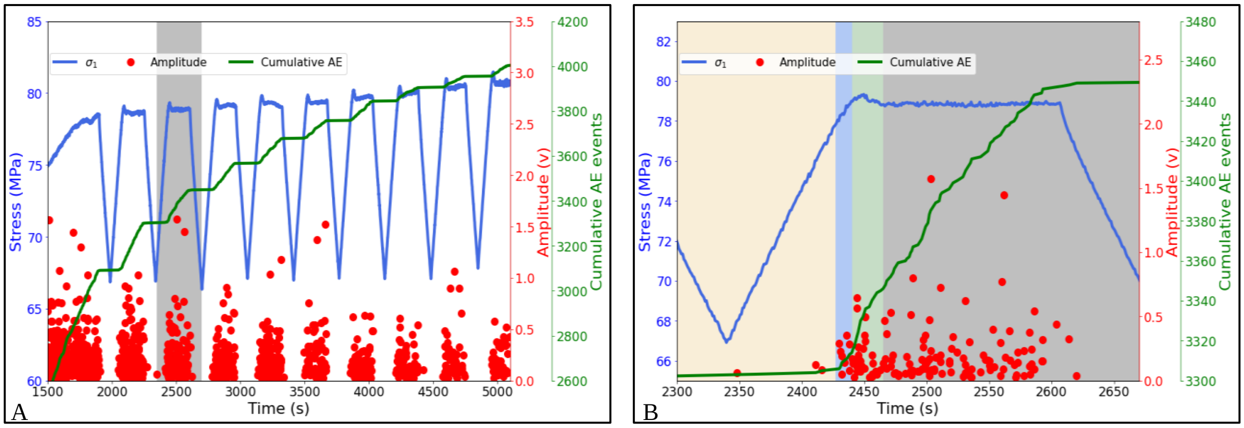

Figure 3: Passive acoustic data (AE) during cycling, showing axial stress ($\sigma1$) as a function of time, and the appearance and amplitude of the single AE events and their cumulative. A. showing all the cycles, the cycle shaded grey is shown in B. showing the different phases of fault reactivation experiment; linear stress build up phase in beige, the pre-slip/ early creep phase in blue, fault reactivation and slip in green, and afterwards in grey the continuous sliding.

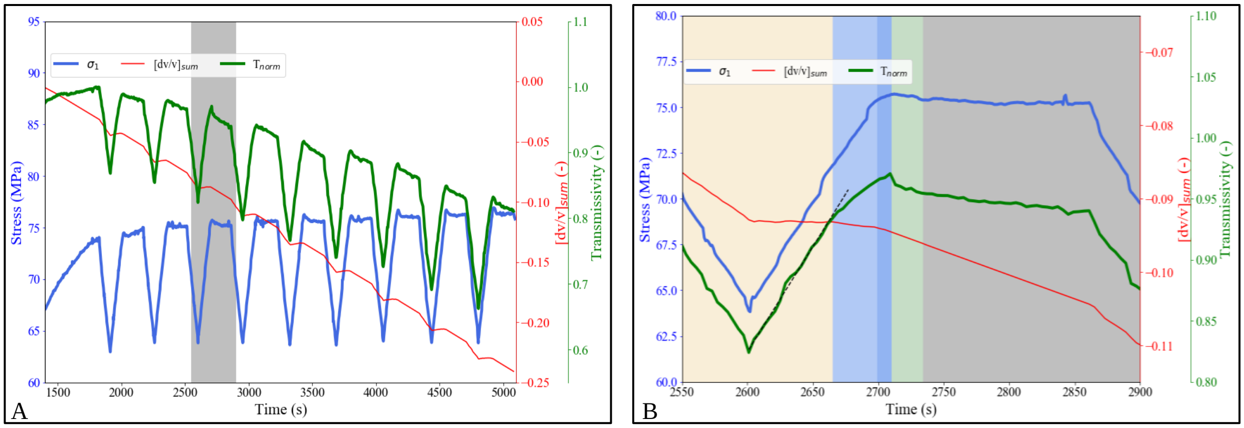

Figure 4: Active acoustic data during cycling, showing axial stress ($\sigma1$) as a function of time, and the changing transmissivity (T) and cumulative velocity change$[\mathrm{dv/v}]_{sum}$ during the cycling, the cycle shaded grey is shown in B. showing the different phases of fault reactivation experiment; linear stress build up phase in beige, the pre-slip/ early creep phase in blue, fault reactivation and slip in green, and afterwards in grey the continuous sliding. Trend line indicates the clear reduction in transmissivity at the start of the pre-slip phase. The pre-slip/ early creep phase in blue has two shades, based on extra decrease in velocity change prior to fault reactivation.